Mem. S.A.It. Vol. 87, 382

Memorie della

Pulsating stars as distance indicators and stellar population tracers

I. Musella

Istituto Nazionale di Astrofisica – Osservatorio Astronomico di Capodimonte, Vicolo Moiariello 16, I-80131 Napoli, Italy, e-mail: ilaria.musella@oacn.inaf.it

Abstract. Pulsating stars can play a fundamental role as distance indicators to set the astronomical distance scale and to trace different stellar populations to infer information on the star formation history of the host galaxy. The most interesting variables are Classical Cepheids and RR Lyrae. A review of the properties of these variables and of the theoretical and observational approaches adopted in the literature are presented.

Key words. Stars: variables – Stars: distances – Stars: Population I– Stars: Population II

1. Introduction

Pulsating stars show a periodic brightness variation. The simplest case is represented by the radial pulsators for which the radius oscillation corresponds to a variation of the star luminosity, with periods ranging from few seconds to many months and amplitudes from few cents to 2-3 mag. Thanks to their light variations and periodic oscillation, variable stars are easier to identify than constant-luminosity stars. In addition, the measurement of their periods and amplitudes is unaffected by reddening and distance uncertainties.

Pulsating stars play an important role in the study of stellar populations and in Cosmology. In fact, their pulsation properties can be used to provide individual and mean distances, to set the extragalactic distance scale through calibration of secondary distance indicators, and to constrain the intrinsic parameters of the associated stellar populations. Depending on their masses, they belong to different evolutionary phases and distinct types of pulsating stars trace stellar generations characterized by different age and chemical composition. The study of different kinds of pulsating stars hosted in a galaxy allow us to trace the intrinsic properties and to define the spatial (3D) distribution of the associated stellar populations. Moreover, pulsating stars can be used to probe the presence of possible radial trends, halos, stream, providing important clues on galactic formation mechanisms. In general pulsating stars offer an alternative route to reconstruct the star formation history (SFH) of the host galaxy, independent and complementary to the color-magnitude diagram (CMD) analysis.

In this context, it is very important not only to rely on accurate observations, but also to adopt a solid theoretical scenario for the pulsation phenomenon. Only through a self-consistent theoretical and observational study of the various pulsation properties, it is possible to put crucial constraints to the evaluation of the evolutionary stellar parameters as well as on the underlying stellar physics (see

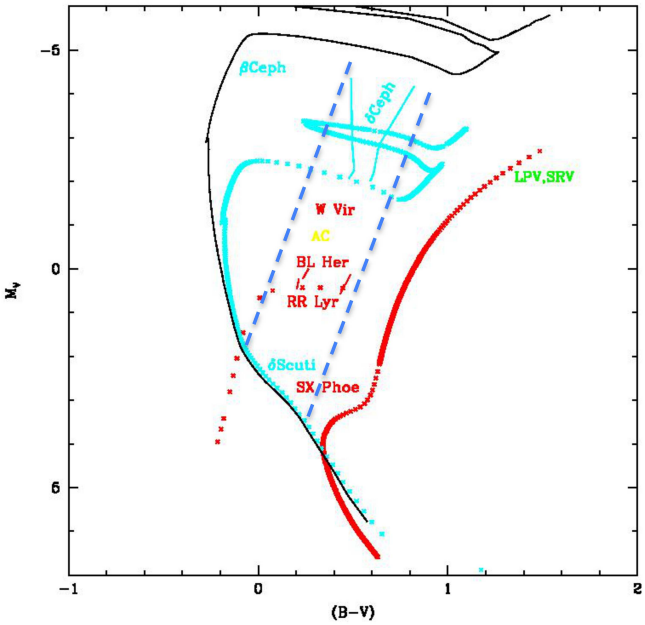

Fig. 1. Location of different types of variable stars in a CMD.

also Marconi 2009, 2012, 2015, and references therein)

2. Pulsating stars as population tracers

Figure 1 shows the location in a Color-Magnitude Diagram (CMD) of different types of variable stars. In the figure we have reported the typical isochrone of a young (cyan) and an old (red) population. Variable stars are located in an almost vertical region of the CMD comprised between the Main Sequence (MS) and the red giant branch. A star passing through this zone, during its evolution, becomes unstable and pulsates. The region between the dashed line is called Instability Strip (IS) and includes variables whose pulsation is based on the same mechanism of variation of the opacity and of the adiabatic exponents (k and γ mechanism, respectively) in the ionization regions of Hydrogen and Helium.

Table 1 summarizes the main properties of the variables in Fig. 1, including the stellar population they belong to and their evolutionary phase. The classes of pulsating stars most used as distance indicators and stellar population tracers are the Classical Cepheids (CCs) and the RR Lyrae (RRs), but also the Population II Cepheids (P2C), the Anomalous Cepheids (ACs) and the SX Phoenicis (SXPhs).

Classical Cepheids (also known as δ Cepheid variables) are metal rich young stars ($t < 100$ Myr) belonging to Population I that, along their evolution, cross the IS during the blue-loop phase. They can be observed in spiral galaxies (see e.g. Freedman et al. 2001; Pietrzyński et al. 2006b; Udalski et al. 2008, 2015, and references therein) and in particular in star-forming regions, thus tracing the youngest stellar generations.

On the other hand, the RRs variables are the Population II low-mass (metal-poor, $t \geq 10$ Gyr, $M < 1 M_{\odot}$) counterparts of CCs. They cross the IS during the Horizontal-Branch (HB) phase, are typically metal-poor, and have been detected in different Galactic

Table 1. Properties of pulsating stars

Class	Period (days)	M_V mag	Population	Evolutionary Phase
δ Cephei (CCs)	$1 \div 100$	$-8 \div -2$	I	Blue loop
δ Scuti	< 0.5	$2 \div 3$	I	Main Sequence/Pre-Main Sequence
β Cephei	< 0.3	$-4.5 \div -3.5$	I	Main Sequence
RV Tauri	$30 \div 100$	$-2 \div -1$	I,II	Post Asymptotic Giant Branch
Miras	> 100	$-2 \div 1$	I,II	Asymptotic Giant Branch
Semiregulars	> 50	$-3 \div 1$	I,II	Asymptotic Giant Branch
RR Lyrae	$0.2 \div 1$	$\sim 0.5 \div 0.6$	II	Horizontal Branch
W Virginis (P2C)	$10 \div 50$	$-3 \div -1$	II	Post-Horizontal Branch
BL Herculis (P2C)	< 10	$-1 \div 0$	II	Post-Horizontal Branch
SX Phoenicis	< 0.1	$2 \div 3$	II	Main Sequence
Anomalous Cepheids	$0.3 \div 2.5$	$-2 \div 0$	?	Horizontal Branch-Turnover

(see e.g. Vivas & Zinn 2006; Drake et al. 2013; Soszyński et al. 2014; Zinn et al. 2014, and references therein) and extragalactic (see e.g. Soszyński et al. 2010; Fiorentino et al. 2012; Cusano et al. 2013, and references therein) environments, including a significant fraction of globular clusters (GCs; see e.g. Coppola et al. 2011; Di Criscienzo et al. 2011; Kuehn et al. 2013; Kunder et al. 2013, and references therein).

Beyond RR Lyrae stars there are three classes of Population II pulsating stars often adopted as distance indicators in the literature.

The so called P2Cs (W Virginis and BL Herculis variables) have a lower mass and a brighter luminosity than RR Lyrae stars, evolve from the very blue part of the Zero Age HB (ZAHB) and show typical periods from ~ 2 to ~ 30 days (see e.g. Marconi& Di Criscienzo 2007; Ripepi et al. 2015, and references therein).

Anomalous Cepheids are more massive (from ~ 1.1 to $\sim 2.2\ M_{\odot}$) and brighter (by ~ 0.5 to ~ 2.0 mag as the period increase from ~ 0.3 to ~ 2 days) than RR Lyrae. They are evolving from the ZAHB turnover (see e.g. Marconi et al. 2004, and references therein), but their origin is still uncertain. The main hypothesis are that 1) they are intermediate-age (≤ 5 Gyr) single stars due to a relatively recent star formation; or 2) they formed from a merging in a binary system of old population stars, thus sharing the same age of the stars from which they originated. In the first hypothesis, the ACs would trace intermediate-age populations ($\sim$ 2-3 Gyr).

SX Phoenicis stars are metal-poor stars in the Main Sequence (MS) and post-MS phases. They show periods of few hours and oscillate both in radial and non radial modes, with a significant fraction of mixed-mode variables (Gilliland et al. 1998). They are currently associated to the so-called oscillating Blue Stragglers and have been the subject of several theoretical (Santolamazza et al. 2001; Fiorentino et al. 2015b) and observational (see Kaluzny & Thompson 2003; Olech et al. 2005; Fiorentino et al. 2014, and references therein) studies. The origin of their pulsation and their actual nature are debated in the literature (see Santolamazza et al. 2001; Fiorentino et al. 2015b, and references therein).

In Fig. 2, we show the various types of variable stars found in the Large Magellanic Cloud (LMC) by the OGLE III Survey (Udalski et al. 2008; Soszynski et al. 2008a; Soszyński et al. 2008b, 2009a,b; Poleski et al. 2010) that allow us to trace different stellar generations in this galaxy.

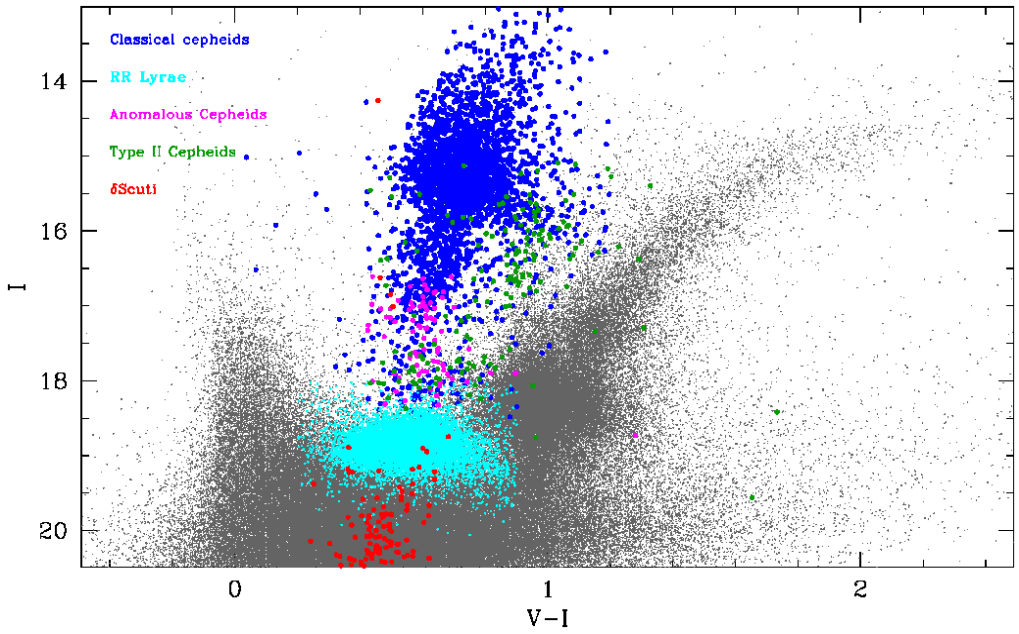

Fig. 2. CMD based on the OGLE III data with the location of the variables found in the LMC by the OGLE III Survey.

3. Pulsating stars as calibrators of the cosmic distance ladder

Classical Cepheids, as population I stars, and RRs, as population II stars, represent the first rung of the cosmic distance ladder. To reach cosmologically significant distances (where the Hubble flow is undisturbed) and to estimate H_0, we need one or more secondary indicators (the Tully-Fisher relation, the Supernovae type Ia based on the CC calibration and the Novae, the Globular Cluster Luminosity Function, the Tip of Red Giant Branch, the Surface Brightness Fluctuations, and the $D_n-\sigma$ based on the RRs calibration).

The physical basis that connects the luminosity and the color of a variable star to its oscillation period is well known. For a pulsating gaseous sphere we have that the product between the square root of the mean density $\rho = 3M/4\pi R^3$ (M is the mass and R is the radius) and the period P is constant ($P\sqrt{\rho} = cost$). For all the stars, the luminosity L can be obtained through the Stefan-Boltzmann law

$$L = 4\pi R^2 \sigma T_e^4$$

where σ is the Stefan-Boltzmann constant and T_e is the effective temperature and σT_e^4 represent the surface area brightness. The Stefan-Boltzmann equation can be converted into observable quantities:

$$M_{BOL} = -5 \log R - 10 \log T_e + C$$

where M_{BOL} is the bolometric magnitude and C is a constant. Moreover, $\log T_e$ and the radius can be mapped through the observables intrinsic color (i.e., $B - V$) and period P, thus obtaining a Period-Luminosity-Color-Mass relation $P = P(L, M, T_e)$ (see Madore & Freedman 1991; Caputo et al. 2000, and references therein, for details). Theory allows us to determine this relation for CCs and RRs.

For example, for LMC fundamental mode CCs Bono et al. (2000), on the basis of their nonlinear convective models, found

$$\log P = 10.557 - 3.28 \log T_e + 0.93 \log L +$$

$$-0.79 \log M$$

Adopting a Mass-Luminosity (ML) relation $L = L(M, Y, Z)$, as predicted by the theory of stellar evolution for Helium burning intermediate mass stars like CCs, in the form

$$\log L = a + b \log M + c \log Z + d \log Y$$

where Z and Y are the metallicity and the helium abundance, respectively, one finally derive a Period-Luminosity-Color (PLC) relation $P = P(L, M, T_e)$. We notice that this PLC relation holds for each individual CC: measuring the period and the color, one infers the absolute magnitude and in turn the distance via the comparison with the observed apparent magnitude. The drawback in the use of this relation is that the observational determination of the color term needs the knowledge of both mean and differential reddening contributions. For these reasons, the relation most commonly used to infer distances with CCs is the Period-Luminosity (PL) relation that is a projection of the PLC on the PL plane: for each magnitude level, the period is averaged over the color extension of the IS. On this basis, the PL relation is a statistical relation: it does not hold for each individual CC, but only for statistical significant CC samples.

Following an analogous procedure, for fundamental RRs, Di Criscienzo et al. (2004) theoretically found

$$\log P = 11.038 - 0.651 \log(M/M_\odot) +$$

$$+0.833 \log(L/L_\odot) - 3.350 \log(T_e) + 0.008 \log Z$$

again on the basis of an extensive and detailed set of nonlinear convective models.

This relation cannot be converted into a PL relation because we cannot rely on a defined ML relation as in the case of CCs. Indeed, as RRs belong to the HB phase, their luminosity is roughly constant in the optical bands, depending only on the metal abundance. A PL relation for RRs is only detected, and predicted, in the NIR filters, as discussed in Section 5.2.

4. Classical Cepheids

Since the discovery by Miss Leavitt (1908, 1912) in the Small Magellanic Cloud (SMC), CCs are known to obey to a PL relation

$$M = a \log P + b$$

where M and P are absolute mean magnitude and period, respectively. If we know the relation between absolute magnitude and period, taking into account that

$$m - M = 5 \log d - 5 + A$$

m, d and A are the apparent magnitude, the distance and the extragalactic absorption, respectively), measuring period and mean apparent magnitude, we can derive the distance.

The PL relation has been traditionally considered "universal" (Iben & Renzini 1984; Freedman & Madore 1990) and not dependent on the host galaxy. For this reason, the calibration of the slope and the zero point was based on the known CCs in the LMC and in the Galaxy, without considering the large metallicity differences between these two galaxies. The advent of the *Hubble Space Telescope* (HST) and of the Key project for the CCs extragalactic distance scale (KP; see e.g. Freedman et al. 2001; Saha et al. 2001, and references therein), with the observation of many galaxies in the Virgo Cluster, with a large spread in metallicity, clearly showed that the CC properties depend on the metallicity of the host galaxy. On this basis, systematic errors in the calibration of the CC distance scale also affect the distance obtained by secondary distance indicators and, in turn, the Hubble constant.

Figure 3 shows, as an example, the PL relations obtained adopting the *BVRIJHK* data for Galactic CCs by Fouqué et al. (2007, magnitudes are manually shifted to avoid an overlap). It points out the increase of the slope and the decrease of the dispersion of the PL relations moving from B to K bands.

Figure 4 shows a CC typical light curve in the *BVRIJK* bands (data from Storm et al. 2004). The amplitude decreases moving from optical to NIR filters. These observational properties imply that CCs are easy to detect in

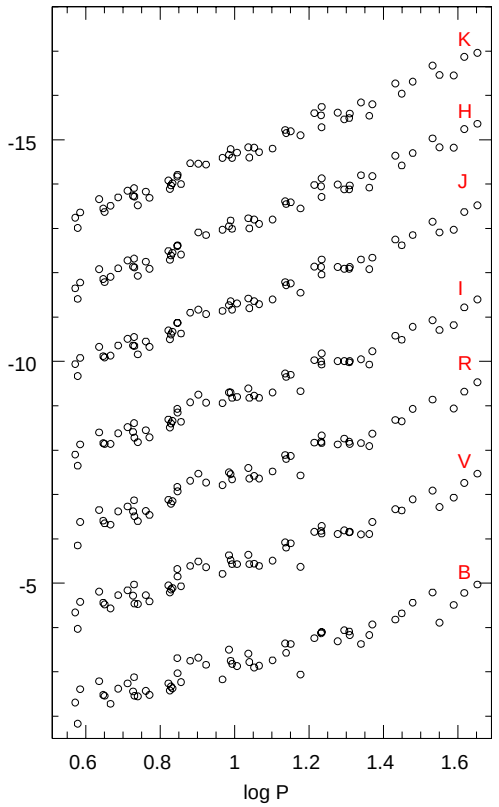

Fig. 3. PL relations obtained adopting the *BVRIJHK* data for Galactic CCs by Fouqué et al. (2007) (see text for details).

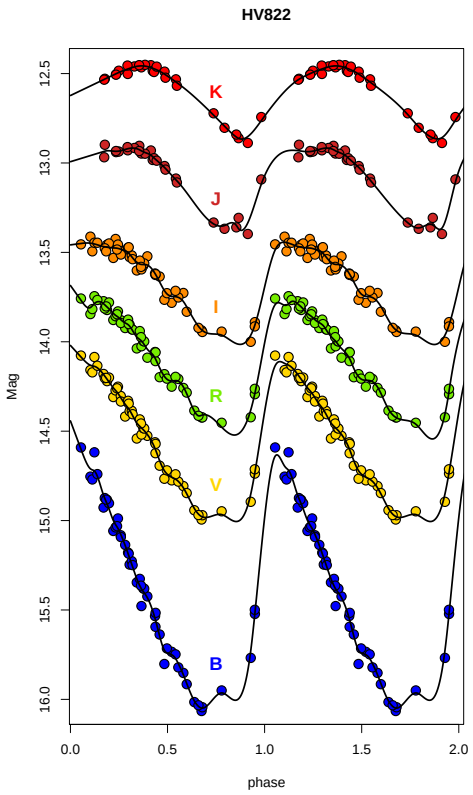

Fig. 4. A typical CC light curve in the *BVRIJK* bands (data from Storm et al. 2004).

the optical bands thanks to their large amplitude, but i) to have a good light-curve coverage in these bands, we need many phase points (telescope time consuming) and ii) the corresponding PL relations have a larger dispersion. On the other hand, in the NIR bands, thanks to the small amplitudes, we need few phase points to get accurate mean magnitudes, but it is very difficult to detect variability. Therefore, we need optical observations to detect the variables and to obtain accurate periods, while NIR observations allow us to obtain more accurate magnitudes and to have intrinsically narrower PL relations.

Moreover, observed and predicted PL relations show evidence of non-linearity with an effect decreasing from optical to NIR bands. In particular, Tammann & Reindl (2002), Sandage et al. (2004), Kanbur & Ngeow (2004) and Ngeow et al. (2005) hypothesized the existence of a break at $P = 10$ d adopting two different slopes for period shorter and longer of 10 d (see, for example, Fig. 4 in Sandage et al. 2004). These empirical results are confirmed by the pulsational models (see below).

On this basis, the problems that can affect the CC distance scale are i) the PL relation dispersion due to the finite width of the IS, the possible differential absorption and the poor sampling of the light curve; ii) the PL relation linearity; iii) the metallicity and reddening effect that can be reach up to 15%; iv) the use of the LMC as reference CC sample due to its large reddening and significant metallicity spread. Possible solution to these problems are i) to have a solid theoretical scenario; ii) obtaining observations in the NIR and Mid

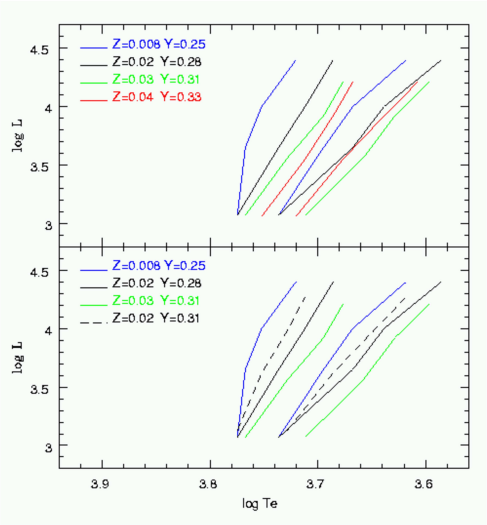

Fig. 5. The CC IS at varying the metallicity and the Helium content.

Infrared (MIR) bands where atmospheric line blanketing and reddening are negligible; iii) to adopt a different anchor galaxy with a metallicity more similar to the galaxies observed by HST. For the last point, a possible reference galaxy is NGC4258 that also has an independent and geometrical measurement of the distance based on a Maser (see e.g. Riess et al. 2011; Fausnaugh et al. 2015, and references therein).

4.1. The theoretical scenario

A solid theoretical scenario can be provided by nonlinear convective pulsational models computed for large ranges of masses (from 3 to 13 $M_{\odot}$) and of chemical compositions ($0.0004 < Z < 0.04$, $0.25 < Y < 0.33$, $0.5 < \Delta Y/\Delta Z < 4$; Fiorentino et al. 2002; Marconi et al. 2005, 2010, and references therein). These models allow us to determine both the blue and the red edge of the IS. It is worth to note that the determination of the red-edge is possible thanks to the time-dependent convection treatment included in these models. Moreover, these models allow us to predict all the observables of the pulsation (periods, amplitudes, mean magnitudes, light-curves, radial velocity curves, and, in general, the variation of any relevant quantity along the pulsation cycle) and, in turn, to simulate CC samples and to build theoretical PL relations in different bands. These relations can be compared with the observed ones to test the models themselves — and refine the physical parameters adopted in the evolutionary and pulsation models — but also to set a theoretical calibration for the CC distance scale and of its dependence on chemical composition.

Figure 5 shows the dependence on the metallicity and Helium content of the IS. In the top panel, we see that at fixed $\Delta Y/\Delta Z$, if Z increases, the IS moves toward lower effective temperature and its width remains quite unchanged except for $Z > 0.03$. The bottom panel shows that, at fixed Z, the effect of a larger Y is to move the IS toward the blue and, at fixed Y, if Z increases, the IS moves toward lower effective temperature. In conclusion, metallicity and helium increases produce opposite trends of the predicted instability strip topology.

To simulate CC samples populating the predicted IS as a function of chemical composition, we populate each IS adopting a fixed number of pulsators (e.g. 1000) and a mass law ($dn/dm = m^{-3}$).

Figure 6 shows the simulated samples built for three different metallicities $Z = 0.004$, 0.008, and 0.02. An inspection of the figure confirms the observational properties listed above (included the non linearity) and shows that the PL relations are dependent on the chemical composition: as Z increases, the PL relation gets flatter and the dependence decreases moving from B to K band (Caputo et al. 2000). On the other hand, Marconi et al. (2010) found that at low metallicity the effect tends to saturate with the PL relations for $Z = 0.0004$ and $Z = 0.004$ being quite similar. This result was also empirically confirmed by Pietrzyński et al. (2006a). The Helium content Y also affects the predicted relations: the slope decreases as Z increases at fixed $\Delta Y/\Delta Z$ and increases as Y increases at fixed Z, but the effect gets significant above $Z \sim 0.008$ (see Marconi et al. 2005; Carini et al. 2014). The theoretical evidence that metal-poor CCs, at fixed period, are brighter than metal-rich ones does not agree with some observational results that find

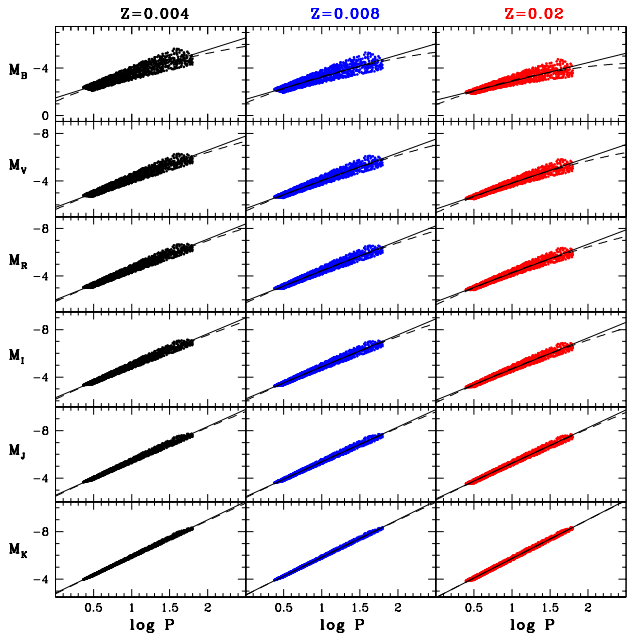

Fig. 6. Theoretical PL relations in the $UBVRIJHK$ bands, obtained for simulated samples at three different metallicities $Z = 0.004, 0.008, 0.02$.

an opposite result. We discuss this point in the following sections.

4.2. The Wesenheit relation

Due to the intrinsic width of the PL, it can be useful to introduce the Wesenheit (WPL) relation (Madore 1982). This is defined as

$$WPL(\lambda_1, \lambda_2) = \lambda_1 - R_{\lambda_1\lambda_2} \times (\lambda_1 - \lambda_2)$$

where λ_i are the bands used and $R_{\lambda_1\lambda_2} = A_{\lambda_1}/E(\lambda_1 - \lambda_2)$ is the ratio of total to selective absorption dependent on the adopted extinction law (see e.g. Cardelli et al. 1989; Fitzpatrick 1999). This relation represents a reddening-free formulation of the PL relation with a reduced intrinsic scatter.

In Fig. 7 are plotted the PL(V), PL(I) and WPL(V-I) relations for the fundamental CCs of OGLE III (Soszynski et al. 2008a). It is evident that the dispersion in the WPL relation is strongly reduced with respect to the PL ones. Figure 8 shows the WPL relations for the simulated samples (based on the pulsational models), for different band combinations and metallicities. The predicted WPL relations are much narrower then the PL ones and with a reduced dependence on chemical composition (well inside the observational errors).

4.3. Empirical tests to determine the metallicity effect

Several tests have been envisaged in the literature to determine the metallicity effect on the CC distance scale.

1. *The comparison between CCs belonging to two fields of different metallicity in the same galaxy.*
   Taking into account that $\Delta \log Z = \Delta[O/H]$, Kennicutt et al. (1998) found that in M101 the metallicity correction for the distance modulus is $\Delta\mu/\Delta[O/H] = -0.24$ mag dex^{-1} and on this basis the

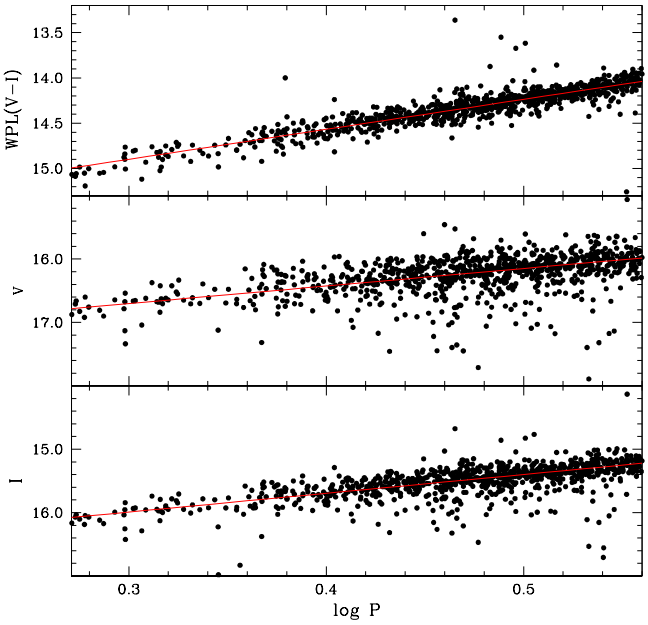

Fig. 7. In the bottom, middle and top panels are plotted the PL(V), PL(I) and WPL(V-I) relations, respectively, for the fundamental CCs of OGLE III (Soszynski et al. 2008a).

KP adopted $\Delta\mu/\Delta[O/H] = -0.2 \pm 0.2$ mag dex^{-1} as metallicity correction (Freedman et al. 2001). In the same galaxy, using different fields, Mager et al. (2013) found $\Delta\mu/\Delta[O/H] = -0.33$ mag dex^{-1}.
On the other hand, Macri et al. (2006), using two different fields in the galaxy NGC4258 that hosts a Maser allowing an independent geometrical (direct) distance estimate, found $\Delta\mu/\Delta[O/H] = -0.33$ mag dex^{-1}.

2. *The comparison between CCs in the two Magellanic Clouds (MCs; see e.g. Sasselov et al. 1997) or between the Magellanic and Galactic pulsators* (see e.g. Kanbur et al. 2003; Storm et al. 2004; Groenewegen et al. 2004; Sandage et al. 2004; Storm et al. 2011).
The results, obtained by these tests, are different from each other both in the value and in the sign of the correction. For example, Storm et al. (2004) found that the Galactic PL relations are flatter than the MC ones while Sandage et al. (2004) found the opposite trend. Such different and controversial results are due to different problems: i) metallicity gradients in galaxies containing CCs are often poorly known. For example, for NGC4258 the various determinations of the gradient available in the literature are very different from each other (Oey & Kennicutt 1993; Zaritsky et al. 1994; Díaz et al. 2000; Bono et al. 2010); ii) blended CCs could be responsible for a large fraction of the distance discrepancy between different fields (see M101 case, Macri et al. 2006); iii) the metallicity difference between the two MCs is small but MC CCs show a non negligible metallicity dispersion; iv) the period range covered by Galactic CCs does not coincide with the ones of the MCs; v) reddening differences can simulate metallicity differences.
3. *The comparison between CC distances and the ones based on methods independent of metallicity.*

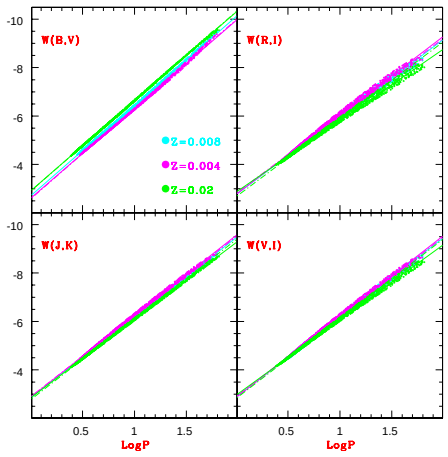

Fig. 8. The WPL relations for the simulated samples, for different band combinations and metallicities.

Using distances obtained from the Tip of Red Giant Branch method (TRGB), Sakai et al. (2004) found $\Delta\mu/\Delta[O/H] = -0.24 \pm 0.05$ mag dex^{-1}, but also in this case, the result strongly depends on the calibration adopted for the TRGB luminosity. In fact, Bono et al. (2008, see their Fig. 12) showed that adopting the calibration of the TRGB by Rizzi et al. (2007) the differences with the CC distance moduli have an opposite trend with respect to that obtained by Sakai et al. (2004).

4.4. Theoretical tests to determine the metallicity effect

From a theoretical point of view, an interesting test is the comparison between the moduli obtained by the KP and those obtained adopting the theoretical pulsational relation for the metallicity of the studied galaxy (Fiorentino et al. 2002; Marconi et al. 2005). The KP adopted, for all the galaxies, the slope of the LMC that has a metallicity very different from that of the HST galaxies, including a metallicity correction on the inferred distance moduli of 0.2 mag dex^{-1}. Fiorentino et al. (2002, see their Fig. 4), using their model predictions, found that neglecting the metallicity correction can introduce an error on the distance modulus up to ± 0.2 mag, and in turn a significant error on the estimated Hubble constant. In addition, Marconi et al. (2005, see their Fig. 10), taking into account both Z and Y (and hence the ratio $\Delta Y/\Delta Z$), found that the metallicity correction depends on the adopted $\Delta Y/\Delta Z$ and on the period range of the CC sample. In particular, the KP empirical correction is reproduced by models for $\Delta Y/\Delta Z = 3.5$. It is worth to note that, the theoretical correction trend is qualitatively in agreement with the result based on spectroscopic [Fe/H] measurement of Galactic (see right panel of Fig. 1 in Romaniello et al. 2005) and Magellanic CCs (Romaniello et al. 2008). Moreover, the application of the theoretical correction to the NGC4258 distance modulus based on the CCs and obtained adopting the LMC slopes in the V and I bands (Newman et al. 2001), gives a result in very good agreement with the geometrical distance determined through the Maser hosted in this galaxy (Caputo et al. 2002).

Finally, we mention the Carnegie Hubble Program (Freedman et al. 2011) that adopts the MIR bands to reduce the systematics due to the metallicity effect, with the final goal to obtain an error of 2% on H_0. The observational dependence on the chemical composition of the Milky Way (Marengo et al. 2010), LMC (Freedman et al. 2008; Ngeow & Kanbur 2008; Madore & Freedman 2009; Ngeow et al. 2009) and SMC (Ngeow & Kanbur 2010) PL relations in these bands appears negligible, but, also in this case, the theoretical models put a warning, showing that the MIR PL slopes for $Z > 0.02$ depend on the metallicity (Ngeow et al. 2012).

4.5. Application of pulsational models to observational samples

In this section, we discuss the application of current nonlinear convective pulsation models to observational samples.

The first example concerns the application of the theoretical Period-Age (PA) and Period-Age-Color (PAC) relations to the SMC and LMC CCs (Bono et al. 2005; Marconi et al.

2006). These relations are obtained by combining stellar evolution and stellar pulsation predictions in a self-consistent theoretical scenario and allow us to determine individual ages for the investigated CCs, as well as their radial distribution in Galactic coordinates. The inferred age distributions show high spatial resolution and provide crucial information about recent star formation episodes in these galaxies.

An interesting second example is the theoretical calibration of the Riess CC sample (Macri et al. 2006; Riess et al. 2009a,b, 2011). In order to obtain an Hubble constant accurate at 3%, Riess et al. (2011) observed, both in the optical and in the NIR bands, with WFC3@HST and ACS@HST, large CC samples in NGC 4258 (used as anchor galaxy to calibrate the distance scale) and in eight galaxies hosting Type Ia Supernovae (SNIa). Transforming the pulsational models in the same photometric filters adopted by Riess et al. (2011), Fiorentino et al. (2013, see their Fig. 4) found for NGC4258 a very good agreement between models and observations, both for the IS and for the PL relations. On the other hand, for the other galaxies of the sample, Fiorentino et al. (2013, see their Fig. 5) found that the farther are the CC samples, the bluer and brighter they appear in comparison with theoretical predictions in the $F160W$-$(V-I)$ plane. This effect could be the sign of an increasing crowding at larger distances. Indeed, when applying the theoretical PL(F160W) relation to the Riess CC samples, the inferred distance moduli are slightly different from those found by Riess et al. (2011) with differences increasing at larger distances (see Fiorentino et al. 2013). Adopting these "theoretical" distance moduli, Fiorentino et al. (2013) found $H_0 = 76.0 \pm 1.9$ km s^{-1}Mpc^{-1} in good agreement with, but with a smaller error than the value found by Riess et al. (2011).

Finally, we mention an investigation of the impact of different CC-based theoretical and empirical calibrations of SNeIa distance scale and, in turn, on H_0 (Altavilla et al. 2004). SNeIa with distances calibrated on the basis of CCs are currently used to calibrate the zero point of the relation between the SNeIa absolute magnitudes and their rate of decline after maximum (Phillips 1993). To determine distances by means of SNeIa, we need to know the host-galaxy extinction and hence to assume an extinction law and a total-to-selective extinction ratio. In this context, Altavilla et al. (2004) found that the Hubble constant, obtained considering different metallicity corrections to the PL relation, different $\Delta Y/\Delta Z$ values and different total-to-selective extinction ratios, range between 68 and 74 km s^{-1} Mpc^{-1}, with associated uncertainties of the order of 10%.

4.6. The Ultra-Long-Period Cepheids and the case of IZw18

To conclude this section on the CCs, it is important to introduce the Ultra Long Period Cepheids (ULPs). The existence of these variables was pointed out by Bird et al. (2009) who identified a number of these variables in nearby star forming galaxies (LMC, SMC, NGC6822, NGC55, NGC300). These variables have light curve very similar to the CC ones, but are 2-4 magnitudes brighter than the CCs. Moreover, they appear to follow the same CC PL and WPL relations (see Figs. 3, 4 and 5 in Bird et al. 2009) and they have been hypothesized to be the counterpart at higher mass and luminosity (and period) of the CCs. It is important to understand the nature of these pulsators because they could represent the "best standard candles" to extend the cosmic distance ladder to $\sim$ 100 Mpc and beyond without using any secondary indicator and reducing the possible errors on the distance determinations and, in turn, on the Hubble constant.

In this context, it is interesting the case of the blue compact galaxy IZw18. This galaxy has the lowest nebular metallicity of all known star forming galaxies, $Z = 1/30 \div 1/50 Z_{\odot}$ (depending on the metallicity scale), a high gas fraction and high star formation rate, producing a blue young stellar population that dominates the integrated luminosity and color suggesting the presence of many CCs. On the contrary, the analysis of ACS@HST data (V and I bands; Aloisi et al. 2007; Fiorentino et al. 2010) shows the presence of only one typical CC with $P = 8.71$ d and of 2 stars with

light-curves very similar to the CCs one, but with very long periods ($P > 100$ d) and very bright magnitudes (high masses). At this low metallicity, evolution and pulsation models do not predict the existence of such massive ULPs (Marconi et al. 2010). Moreover, the lacking of expected CCs with P in the range $10 \div 100$ d suggests the star-bursting nature of this galaxy: very active in recent epochs but without a significant star formation in the epoch in which the missing CCs (stars with a mass from 6 to 20 $M_{\odot}$) should have formed (Aloisi et al. 2007; Contreras Ramos et al. 2011; Annibali et al. 2013).

As we point out above, pulsational models indicate that the predicted metallicity effect saturates toward low metallicity ($Z < 0.004$). Then, such type of very low metallicity galaxies could be an alternative to supermetallic HST spirals adopted to calibrate the CC distance scale (Marconi et al. 2010). Moreover, If the ULPs were confirmed to be the extension of CCs to higher masses, they would provide key constraints on the input physics of evolution and pulsation models of massive stars (Marconi et al. 2010).

5. RR Lyrae

As we said above, RR Lyrae are low mass helium burning stars, on the HB in the HR diagram. Their properties are summarized in Table 1.

They are the most abundant class of pulsating stars in the Milky Way (MW) and are found both in the field and in globular clusters (GCs) and, thanks to their characteristic light-curve, are easy to detect. As pointed out in section 2 they are important tracers of the chemical and dynamical properties of old stellar populations and hence they can provide hints on galactic formation and evolutionary mechanisms.

RRs are also distance indicators through the $M_V(RR) - [Fe/H]$ relation in the optical bands and the Period-Luminosity relation in the NIR bands. Indeed, they can be used to determine the distance of old systems, and to map the 3D distribution of the stars and the possible presence of radial trends, halos and stream (see e.g. Vivas & Zinn 2006; Marconi et al. 2014, and references therein).

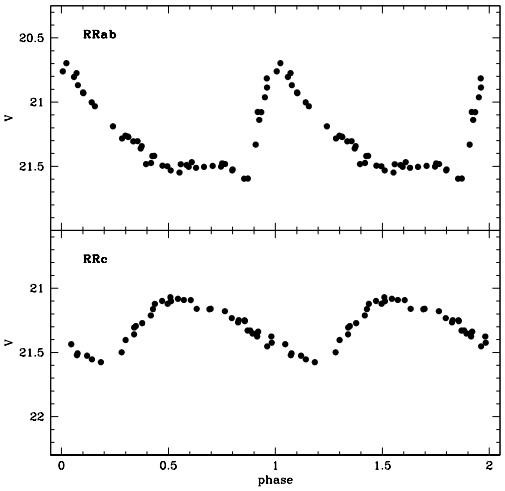

Fig. 9. The typical light curves of a RRab and of a RRc are plotted in the top and in the bottom panel, respectively.

It is possible to distinguish between ab-type RRs (RRab), characterized by an asymmetric light curves (top panel of Fig. 9) and c-type RRs (RRc), with an almost sinusoidal light-curve (bottom panel of Fig. 9).

The RRab have amplitudes decreasing as the pulsation period increases, while the RRc have shorter periods and smaller amplitudes than RRab as shown in the Period-Amplitude diagram (called Bailey diagram) in Fig. 10. RRab and RRc occupy two distinct regions of this diagram with the RRab showing a linear behavior and the RRc depicting a bell shape. We know from the pulsation theory that RRab correspond to fundamental pulsators and RRc to first overtone variables.

Moreover, some RRs show a double-mode behavior, pulsating simultaneously in the fundamental and in the first overtone mode, and are called d-type RRs (RRd). These are particularly useful to constrain the stellar mass through the analysis of the ratio between the first overtone and the fundamental period (see e.g. Marconi et al. 2015; Coppola et al. 2015, and references therein).

Finally, a significant fraction of RRs is affected by the Blazhko phenomenon, that is a

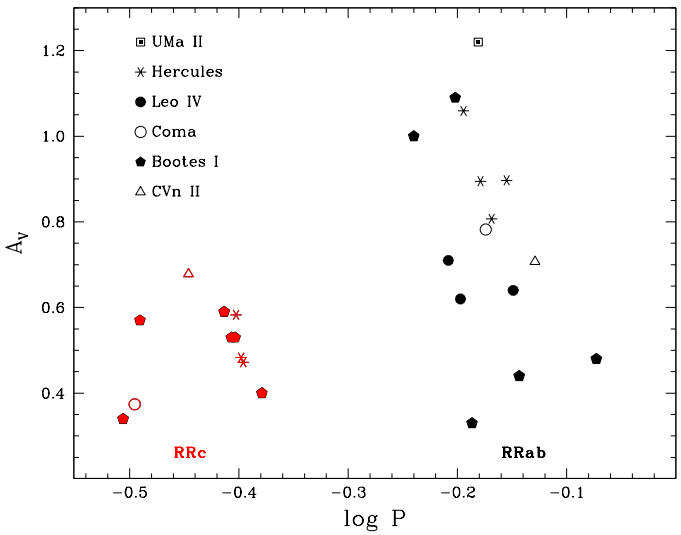

Fig. 10. A typical amplitude-period diagram.

long-period modulation with a variation in amplitude and period. The origin of this effect is still debated in the literature (see e.g. Kovács 2009, and references therein)

5.1. The theoretical scenario

We need accurate pulsation models to reproduce and interpret the observed properties of RRs and to calibrate the cosmic distance scale based on these pulsators. Again, only nonlinear convective models are able to reproduce all the used pulsational observables (periods, amplitudes, blue and red edges of the IS; Bono & Stellingwerf 1994; Bono et al. 1997; Marconi et al. 2003; Di Criscienzo et al. 2004; Marconi et al. 2011, 2015).

On this basis, accurate theoretical tools have been developed to constrain both the distance and the intrinsic stellar parameters of the investigated pulsators (see e.g. Bono et al. 2000, 2003; Di Criscienzo et al. 2004; Marconi& Clementini 2005; Marconi et al. 2015, and references therein). For example, from the relation connecting the period to the mass, the luminosity and the effective temperature given in Section 3, Di Criscienzo et al. (2004) derived a metal-dependent Period-Magnitude-Color-Mass (PMC) relation

$$\log P = -0.34 < M_V > -0.54 \log(M/M_\odot) + \\ + a(Z) + b(Z)[< M_B > - < M_V >]$$

and a Period-Magnitude-Amplitude-Mass (PMA) relation

$$\log P = -0.38 < M_V > -0.30 \log(M/M_\odot) + \\ + 0.13 - 0.189 A_V$$

Given a sample of RRs, sharing the same distance, reddening and metallicity (e. g. in a GC) and with measured periods and colors, the PMC relation allows us to estimate the mass range with an uncertainty lower than 2%. If independent estimates of the cluster distance and metallicity are available, we can also determine the absolute value of the masses. On the contrary, if we know mass, reddening and metallicity for a sample of RRs, measuring period and color, we can obtain the individual distances. In the same way, by applying the PMA relation to a sample with measured periods and amplitudes, we can obtain information on the stellar mass if the distance is known, or on the distance if the mass is known.

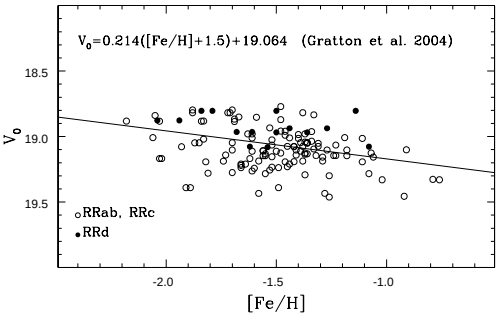

Fig. 11. $M_v - [Fe/H]$ relation obtained for LMC RRs, obtained on the basis of the data by Gratton et al. (2004).

5.2. RR Lyrae as distance indicator

As mentioned above RRs do not obey to a PL relation in the optical bands. Their nature of standard candles is traditionally associated to a relation between the absolute V magnitude and the metal abundance $[Fe/H]$:

$$M_V(RR) = a + b[Fe/H].$$

This relation is adopted to infer distances to GCs or nearby galaxies containing RRs. An example is showed in Fig. 11 for LMC RRs, obtained on the basis of the data by Gratton et al. (2004). In the literature one can find many different values for the slope and the zero-point of this relation with a ranging from 0.13 to 0.30 and b from 0.5 to 1.0. An accurate knowledge of a and b is also crucial to get information on the absolute and relative ages of GCs respectively and, in turn, to understand the formation and evolution of the GCs (see e.g. Cassisi et al. 1999; VandenBerg et al. 2013, and references therein).

Current nonlinear convective pulsation models (Caputo et al. 2000) predict that this relation is not linear over the whole metallicity range covered by Galactic GCs and this prediction is also confirmed by evolutionary models (see e.g. Cassisi et al. 1999; Demarque et al. 2000; Catelan et al. 2004) and by empirical results supporting a cutoff at $[Fe/H] = -1.5$ dex (Rey et al. 2000).

The large uncertainties in the calibration of the slope and zero-point of the $M_v - [Fe/H]$ relation are due to many unresolved issues:

i) the definition of $M_v(RR)$: can it be associated to the lower envelope of the RRs distribution, to the average magnitude of the observed RRs or to any other level?
ii) the ZAHB luminosity dependence on the helium abundance;
iii) the evidence that many observed RRs are evolved from the ZAHB: at fixed chemical composition, this evolutionary effect, is of about 0.1 mag for the RRs evolving from the red boundary of the IS, but can reach ∼0.4 mag for RRs evolving from the blue boundary;
iv) the transformation from the measured abundance $[Fe/H]$ to the global metallicity Z adopted in the stellar models.

All these uncertainties put limits to use this relation as standard candle. On the other hand, since 1986 (Longmore et al. 1986, 1990), it has become clear that RRs obey to a PL relation in the NIR bands. The distribution of a sample of RRs in the logP-magnitude plane from the B to the K band is clearly shown in Catelan et al. (2004) (see their Fig. 2). A linear relation only exists in the NIR bands and in particular in the K filter where it shows the smallest dispersion. Figure 12 shows a very recent PL(K) obtained for a sample of RRs in the LMC, in the framework of the VMC survey (Muraveva et al. 2015, and references therein). The PL(K) relation has several advantages over the $M_v - [Fe/H]$ relation. The reddening effect is smaller in K than in V and the period is much easier to measure than $[Fe/H]$. Moreover, the above mentioned evolutionary effects are significantly reduced in the K band (see discussion in Bono et al. 2001) Therefore, if the metallicity effect is small and/or accurately known (see discussion below), by applying the PL(K), we can get accurate distances to the observed stellar systems.

From the theoretical point of view, the physical basis of the existence of a NIR PL for RRs is well known. We know that in the HB phase the visual magnitude is independent of

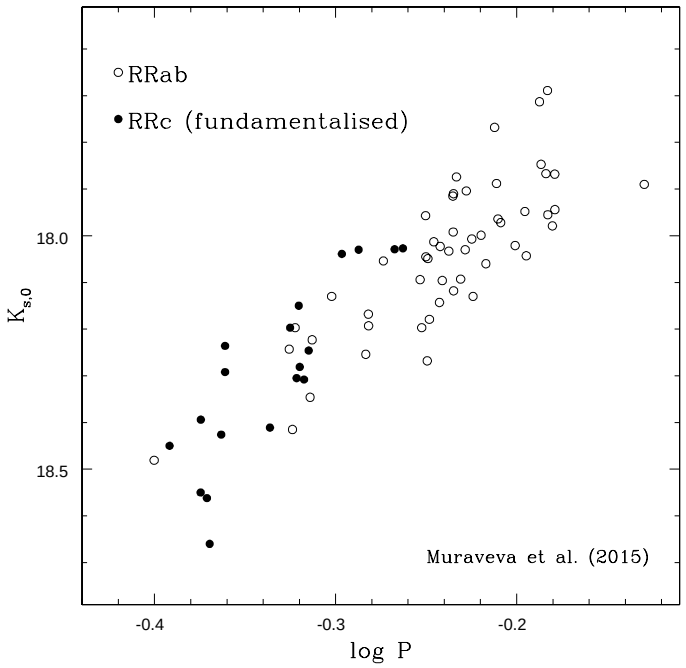

Fig. 12. The PL(K) relation obtained for a sample of RRs in the LMC in the framework of the VMC survey (Muraveva et al. 2015).

both the effetive temperature (T_e) and the pulsation period, while, as shown in Fig. 13, the period and the color $V - K$ are dependent on T_e.

For this reason, as shown in Fig. 14, the relation between the visual magnitude and the period (at fixed metallicity) depends only on the assumed luminosity level, while the relation between K and $\log P$ is linear with a very small dependence on the luminosity level, and in turn on evolutionary effects (Bono et al. 2001).

On the other hand, the PL(K) shows a non negligible dispersion related to a metallicity effect. Correcting for the metallicity and the small evolutionary contributions, the dispersion of the predicted distributions of RRs in the $M_K - \log P$ becomes significantly smaller (see Fig. 3 in Bono et al. 2001). Indeed the "true" relation is not a PL(K) but a PLZ(K):

$$M_K = a + b \log P + c[Fe/H]$$

The dispersion of the PLZ(K) is very small (σ~0.05 mag), but the coefficient of the metallicity term is debated in the literature. For example, Bono et al. (2003) found:

$M_K = -0.77 - 2.101 \log P + 0.231[Fe/H]$,

Catelan et al. (2004):

$M_K = -0.597 - 2.353 \log P + 0.175[Fe/H]$,

Sollima et al. (2008):

$M_K = -1.07 + -2.38 \log P + 0.08[Fe/H]$,

and, recently, Muraveva et al. (2015):

$M_K = -0.95 + -2.53 \log P + 0.07[Fe/H]$.

Muraveva et al. (2015) also analyze the theoretical and empirical dependence on Z of the PL(K) in different systems in the MW and in the LMC, suggesting a mild dependence on Z of this relation. Dall'Ora et al. (2004) and Szewczyk et al. (2008) give two calibrations of the LMC distance based on the PLZ(K) relation obtaining 18.52 ± 0.005(rand)± 0.117(sys) mag and 18.58 ± 0.03(stat)± 0.11(sys) mag that are in good agreement with most independent determinations.

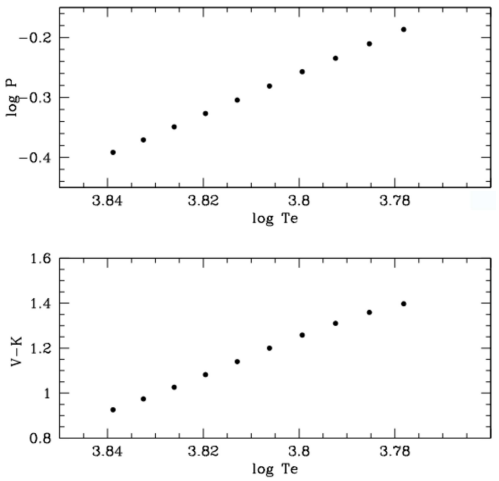

Fig. 13. The dependence of $\log P$ and of the color $V-K$ on the effective temperature T_e are plotted in the top and in the bottom panel, respectively.

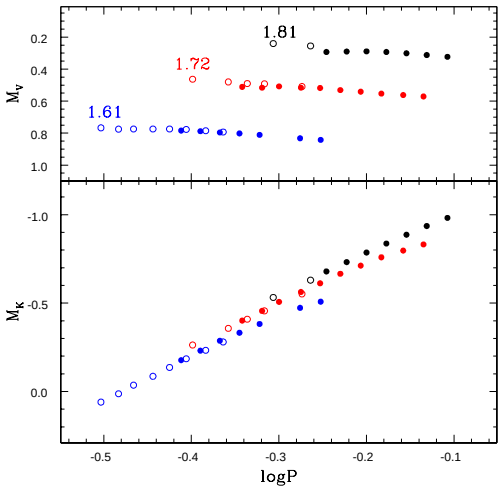

Fig. 14. The relation between the V and K magnitude and the period are plotted in the top and bottom panel, respectively.

5.3. RR Lyrae as stellar population tracers

As mentioned above, RRs can also be used to investigate the formation and the evolution of the MW Halo and to understand the possible candidates to be the hypothesized Building Blocks of the MW (Searle & Zinn 1978).

The main scenario for the galaxy formation are the monolithic cloud collapse, the merging (that is a hierarchical formation of the galaxies) or a possible combination of these two processes. In particular, the Λ-CMD hierarchical scenario hypothesizes dwarf Spheroidal galaxies (dSphs) as building blocks of larger galaxies (such as the MW), so we expect to see evidence of this process and to find that the properties of the MW halo are homogeneous with those of the MW dSph satellites. We have many observational examples of merging in recent large scale surveys that discovered streams and substructures in the MW and M31 halo (see e.g. Belokurov et al. 2006, 2010; Richardson et al. 2011, and references therein).

Fiorentino et al. (2015a) studied the role of dSphs in the Galactic halo formation using amplitudes and periods (that are reddening independent quantities) of observed RRs. Indeed, the fundamental RRs observed in all the dSphs (apart from Sagittarius) do not include any HASP (High Amplitude Short Period, $P <$ 0.48 d) variable. These RRs are instead observed in the Galactic halo, in GCs and in massive dwarf irregular galaxies as LMC and Sagittarius (see Fig. 1 in Fiorentino et al. 2015a). The analysis of the RRs samples in 2 LMC and 16 MW GCs covering a large range in metallicity $-2.3 < [Fe/H] < -1.1$ dex showed that there is no HASP variable for $[Fe/H] < -1.5$ dex (see Fig. 2 in Fiorentino et al. 2015a) and the maximum metallicity of the RRs observed in dSphs is about -1.5 dex. On this basis, the dSphs do not appear to be the building blocks of the Galactic halo. On the other hand, massive irregular dwarfs with a large spread in metallicity and an old population (e.g. LMC, Sagittarius) could have contributed to the halo formation.

The study of RRs is very interesting to understand the star-formation history of the MW halo. In fact, in the MW the GCs can be divided in two classes on the basis of the properties of their RRs population. If the mean period of the RRab is 0.55d and the number of RRab is significantly higher than the number of RRc we have an Oosterhoff I (OoI) cluster, while if $<$ P_{ab} $>=$ 0.65 d and the number of RRab is sim-

ilar to number of RRc, we have an Oosterhoff II (OoII) type. For the MW GCs, we have a sharp division, with very few clusters with mean periods ranging in the interval between 0.58 and 0.62 d, called Oosterhoff gap, with the GCs in this region defined as Oosterhoff intermediate (OoInt). Even if we analyze the field MW halo RRs, we find that a significant part has a typical OoII period (Oluseyi et al. 2012). On the other hand, the GCs belonging to the classical dSphs and the Magellanic Clouds are preferentially classified as OoInt falling in the Oosterhoff gap. For these additional reasons, it is very difficult to hypothesize the classical dwarf galaxies as the building blocks of the MW halo.

In the last few years, many new satellites of the MW (see e.g. Belokurov et al. 2006, 2010, and references therein) and M31 (see e.g. Richardson et al. 2011, and references therein) have been discovered. The new MW satellites represent a new type of dwarf galaxies characterized by similar or lower size than classical dwarf, but with a surface brightness lower than expected (see e.g., Fig. 1 in Clementini et al. 2012). For this reason, they are called Ultra Faint Dwarfs (UFDs). Many of these new galaxies in the MW were discovered from the analysis the Sloan Digital Sky Survey data.

UFDs are fainter than previously known dwarf galaxies and have properties intermediate between GCs and dSphs. Moreover, they show a very irregular shape, probably due to the tidal interaction with the MW halo. They appear to be characterized by an old stellar population as metal poor as the MW halo stars and with a large metallicity dispersion. Their CMD is very similar to metal-poor Galactic GCs as M15, M68, M92 and they generally host RR stars. Most of the UFDs (except the peculiar UFDs CVnI and Leo T) are OoII type (Dall'Ora et al. 2006; Kuehn et al. 2008; Greco et al. 2008; Musella et al. 2009; Moretti et al. 2009; Dall'Ora et al. 2012; Musella et al. 2012; Clementini et al. 2012; Garofalo et al. 2013, and references therein) showing characteristics similar to those expected for the building blocks of the MW halo.

6. Variable stars surveys

There are many stellar survey that use variables as stellar population tracers and distance indicators. Here, I only mention some of them.

The QUEST survey (Vivas & Zinn 2006) searches RRs overdensities in the Galactic halo that may be stellar streams or debris from destroyed satellite galaxies. This survey has covered about 700 sq. deg. of the sky, detecting ~700 RRs, covering all the metallicity range and different environments, from the inner and outer Galactic halo to all the dSphs and GCs. In this framework, several overdensities were found, among which the most prominent is the northern tidal stream left by the Sagittarius dwarf spheroidal galaxy.

Another interesting project searching for stellar stream and/or extended halo around dSphs and GCs is the ongoing survey STREGA@VST (see Marconi et al. 2014, and references therein).

In the context of the OGLE III (Udalski et al. 2008) and OGLE IV (Udalski et al. 2015) survey, it has been studied the distribution of the CCs and of the the RRs in the LMC. The map of detected RRs traces the bar and the inclination of the disk (see Fig. 6 in Soszyński et al. 2009a) and show an highest density towards the center, indicating that most of these variables formed in the disk. On the basis of this analysis, Subramaniam & Subramanian (2009) suggest that a major star forming event happened in the LMC at 10-12 Gyrs ago, possibly a merger with a gas rich galaxy, resulting in the formation of most of the RRs and probably of the GCs and of the LMC disk. On the other hand, the distribution of the CCs, identified in the OGLE III catalog, is elongated with the high density along the LMC bar (see Fig. 4 in Soszynski et al. 2008a). The distribution is not homogeneous, but show different regions of overdensities that trace the star forming region during the past 30 ÷ 300 Myr (see e.g Grebel & Brandner 1998)

Another interesting survey is the VMC (Vista Magellanic Cloud) survey that is a VISTA@ESO photometric public survey (P.I.: M.R. Cioni). This survey covers 116 sq. deg. on the LMC, 45 sq. deg. on the SMC and 20 sq.

deg. on the Bridge between the two MCs in the NIR bands and is specifically designed to have a good sampling of RR and CC light curves (Cioni et al. 2011). For this survey, the light curves for RRs and CCs in the optical bands are obtained by the EROS (Tisserand et al. 2007) and OGLE III (Soszynski et al. 2008a; Soszyński et al. 2009a) surveys for LMC and SMC galaxies and by the STEP@VST survey for the Bridge. In the two fields analyzed so far (Ripepi et al. 2012; Muraveva et al. 2015), it has been possible to determine the difference in distance between these two fields thanks to the use of the Wesenheit relation for the CCs and the PL$Z(K)$ for the RR Lyrae. These tracers are ideal to do a 3D map of the MCs.

Finally, the largest NIR data-set for the CCs in the MCs was obtained by (Inno et al. 2013) using the optical light curves by OGLE III. They confirm (see their Fig. 2) the theoretical results of a Wesenheit relations with a negligible dependence on the metallicity and show the possibility to use these variables to trace the geometrical stellar distribution in the MCs.

7. Model fitting of observed light, radial velocity and radius curves

An additional method to get distances with CCs and RRs is represented by the model fitting of the observed variations of luminosity but also radial velocity or radius along a pulsation cycle. As stated above, nonlinear convective models predict accurately these variations. A direct comparison between predicted and observed light (but if available also radial velocity and/or radius curves) allows us to directly infer the intrinsic stellar parameters and the individual distances of the investigated pulsators. The first application of this method was presented by Wood et al. (1997) for a LMC CC using the V and I light curves. A subsequent application to an RR star by Bono et al. (2000) (see their Fig. 2), using $UBVK$ light curves gives tight constraints on the intrinsic stellar parameters of this star (mass, effective temperature, gravity) and on its distance. The application of this model fitting method to three different class of variable stars in the LMC, specifically CC (Bono et al. 2002), RR (Marconi& Clementini 2005) and δ Scuti (McNamara et al. 2007) stars, gives distances in agreement with each other and with independent results obtained by Keller & Wood (2002, 2006) based on their model fitting of MACHO CCs.

If the radial velocity curve is available too, it is possible to simultaneously fit light and radial velocity curves (see e.g. Fig. 10 in Di Fabrizio et al. 2002). In Natale et al. (2008) this method is applied to the prototype δ *Cephei* using not only the light and the radial velocity, but also the radius curve (see their Figs. 1 and 2). It is worth to note that the optical light curves depend on the surface temperature and the radius variation and that the dependence on temperature is reduced in the NIR bands. The radial velocity is independent of the reddening, but it depends on the debated *p-factor* used to transform the radial velocity into the pulsation velocity. Finally, the radius curve is independent of both reddening and *p-factor* uncertainties. This model fitting technique was recently applied to the light, radial velocity and radius curves of an OGLE CC belonging to the eclipsing binary in the LMC (OGLE-LMC-CEP0227; Marconi et al. 2013) for which Pietrzyński et al. (2010) had given a dynamical estimate of the mass with an unprecedented precision of 1%. Marconi et al. (2013) using the model fitting obtained a very good agreement between pulsational model and dynamical estimates of the stellar parameters, thus supporting the predictive capabilities of the adopted theoretical scenario.

8. The Gaia mission

As discussed above, thanks to the relation between pulsation and intrinsic stellar parameters, pulsating stars can be used as stellar population tracers and distance indicators. Moreover, thanks to updated nonlinear convective hydrodynamic models we are able to theoretically reproduce all the relevant pulsation observables. In spite of this encouraging framework, the results discussed in the previous sections clearly show that there are still open issues in the use of CCs and RRs as standard candles. The solution of at least some of these problems is expected from the large

amount of very accurate stellar distances provided by the astrometrical satellite *Gaia*, that has been launched at the end of 2013 and will provide the first data release towards the mid-2016.

To have an idea of the impressive step forward expected from Gaia, note that at the moment we rely on ~800 MW known CCs (ASAS catalog; Pojmanski 2002) mainly near the Sun, while thanks to the Gaia mission, we expect to observe up 9000 CCs and to obtain parallaxes with errors less than 3% for about 7000. Moreover, in the LMC and SMC we count 3361 and 4630 (respectively) CCs, observed by OGLE III. For about 400 of these variables, Gaia will obtain parallaxes with errors less than 7-8%.

As for the RRs, actually, we know 16836 pulsators in the MW from OGLE III (Soszyński et al. 2011). The Gaia mission is expected to observe up to 15000-40000 RRs in the bulge and 70000 in the Galactic halo: it will be decupled the number of known Galactic RRs. The expected errors on the parallaxes are less than 1% and 2.5% within 1.5 and 3 kpc, respectively, and about 25-30% at 10 kpc. Therefore, we will know RRs in the Galactic GCs with $\sigma\pi/\pi < 1\%$. On this basis, we will have a tridimensional map, extremely precise, of the variable stars in the MW and MCs from which we will derive information about the origin and the evolution of these systems. Moreover, coupling direct trigonometric distances for CCs and RRs and accurate spectroscopic metallicities, it will be possible to get an accurate calibration for the CC PL and of the RRs luminosity, and in turn of the cosmic distance scale.

Acknowledgements. I'm grateful to Marcella Marconi who has worked with me on many aspects presented in this review.

References

Aloisi, A., Clementini, G., Tosi, M., et al. 2007, ApJ, 667, L151
Altavilla, G., Fiorentino, G., Marconi, M., et al. 2004, MNRAS, 349, 1344
Annibali, F., Cignoni, M., Tosi, M., et al. 2013, AJ, 146, 144
Belokurov, V., Zucker, D. B., Evans, N. W., et al. 2006, ApJ, 647, L111
Belokurov, V., Walker, M. G., Evans, N. W., et al. 2010, ApJ, 712, L103
Bird, J. C., Stanek, K. Z., & Prieto, J. L. 2009, ApJ, 695, 874
Bono, G., & Stellingwerf, R. F. 1994, ApJS, 93, 233
Bono, G., et al.1997, ApJ, 479, 279
Bono, G., Castellani, V., & Marconi, M. 2000, ApJ, 532, L129
Bono, G., et al. 2001, MNRAS, 326, 1183
Bono, G., Castellani, V., & Marconi, M. 2002, ApJ, 565, L83
Bono, G., Caputo, F., Castellani, V., et al. 2003, MNRAS, 344, 1097
Bono, G., Marconi, M., Cassisi, S., et al. 2005, ApJ, 621, 966
Bono, G., et al. 2008, ApJ, 684, 102
Bono, G., Caputo, F., Marconi, M., & Musella, I. 2010, ApJ, 715, 277
Bono, G., Castellani, V., & Marconi, M. 2000, ApJ, 529, 293
Caputo, F., et al. 2000, MNRAS, 316, 819
Caputo, F., Marconi, M., & Musella, I. 2000, A&A, 354, 610
Caputo, F., Marconi, M., & Musella, I. 2002, ApJ, 566, 833
Cardelli, J. A., Clayton, G. C., & Mathis, J. S. 1989, ApJ, 345, 245
Carini, R., et al. 2014, A&A, 561, A110
Cassisi, S., et al. 1999, A&AS, 134, 103
Catelan, M., Pritzl, B. J., & Smith, H. A. 2004, ApJS, 154, 633
Cioni, M.-R. L., Clementini, G., Girardi, L., et al. 2011, A&A, 527, A116
Clementini, G., Cignoni, M., Contreras Ramos, R., et al. 2012, ApJ, 756, 108
Contreras Ramos, R., Annibali, F., Fiorentino, G., et al. 2011, ApJ, 739, 74
Coppola, G., Dall'Ora, M., Ripepi, V., et al. 2011, MNRAS, 416, 1056
Coppola, G., Marconi, M., Stetson, P. B., et al. 2015, ApJ, 814, 71
Cusano, F., Clementini, G., Garofalo, A., et al. 2013, ApJ, 779, 7
Dall'Ora, M., Storm, J., Bono, G., et al. 2004, ApJ, 610, 269
Dall'Ora, M., Clementini, G., Kinemuchi, K., et al. 2006, ApJ, 653, L109

Dall'Ora, M., Kinemuchi, K., Ripepi, V., et al. 2012, ApJ, 752, 42
Demarque, P., et al. 2000, AJ, 119, 1398
Díaz, A. I., et al. 2000, MNRAS, 318, 462
Di Criscienzo, M., Marconi, M., & Caputo, F. 2004, ApJ, 612, 1092
Di Criscienzo, M., Greco, C., Ripepi, V., et al. 2011, AJ, 141, 81
Di Fabrizio, L., Clementini, G., Marconi, M., et al. 2002, MNRAS, 336, 841
Drake, A. J., Catelan, M., Djorgovski, S. G., et al. 2013, ApJ, 763, 32
Fausnaugh, M. M., Kochanek, C. S., Gerke, J. R., et al. 2015, MNRAS, 450, 3597
Fiorentino, G., et al. 2002, ApJ, 576, 402
Fiorentino, G., Contreras Ramos, R., Clementini, G., et al. 2010, ApJ, 711, 808
Fiorentino, G., et al. 2012, A&A, 539, A138
Fiorentino, G., Musella, I., & Marconi, M. 2013, MNRAS, 434, 2866
Fiorentino, G., Lanzoni, B., Dalessandro, E., et al. 2014, ApJ, 783, 34
Fiorentino, G., Bono, G., Monelli, M., et al. 2015, ApJ, 798, L12
Fiorentino, G., Marconi, M., Bono, G., et al. 2015, ApJ, 810, 15
Fitzpatrick, E. L. 1999, PASP, 111, 63
Fouqué, P., Arriagada, P., Storm, J., et al. 2007, A&A, 476, 73
Freedman, W. L., & Madore, B. F. 1990, ApJ, 365, 186
Freedman, W. L., Madore, B. F., Gibson, B. K., et al. 2001, ApJ, 553, 47
Freedman, W. L., et al. 2008, ApJ, 679, 71
Freedman, W. L., Madore, B. F., Scowcroft, V., et al. 2011, AJ, 142, 192
Garofalo, A., Cusano, F., Clementini, G., et al. 2013, ApJ, 767, 62
Gilliland, R. L., Bono, G., Edmonds, P. D., et al. 1998, ApJ, 507, 818
Gratton, R. G., Bragaglia, A., Clementini, G., et al. 2004, A&A, 421, 937
Grebel, E. K., & Brandner, W. 1998, in The Magellanic Clouds and Other Dwarf Galaxies, T. Richtler, J. M. Braun eds. (Shaker Verlag, Aachen), 151
Greco, C., Dall'Ora, M., Clementini, G., et al. 2008, ApJ, 675, L73
Groenewegen, M. A. T., et al. 2004, A&A, 420, 655
Iben, I., & Renzini, A. 1984, Phys. Rep., 105, 329
Inno, L., Matsunaga, N., Bono, G., et al. 2013, ApJ, 764, 84
Kaluzny, J., & Thompson, I. B. 2003, AJ, 125, 2534
Kanbur, S. M., et al. 2003, A&A, 411, 361
Kanbur, S. M., & Ngeow, C.-C. 2004, MNRAS, 350, 962
Keller, S. C., & Wood, P. R. 2002, ApJ, 578, 144
Keller, S. C., & Wood, P. R. 2006, ApJ, 642, 834
Kennicutt, R. C., Jr., Stetson, P. B., Saha, A., et al. 1998, ApJ, 498, 181
Kovács, G. 2009, AIP Conf. Series, 1170, 261
Kuehn, C., Kinemuchi, K., Ripepi, V., et al. 2008, ApJ, 674, L81
Kuehn, C. A., Dame, K., Smith, H. A., et al. 2013, AJ, 145, 160
Kunder, A., et al. 2013, AJ, 145, 33
Longmore, A. J., Fernley, J. A., & Jameson, R. F. 1986, MNRAS, 220, 279
Longmore, A. J., et al. 1990, MNRAS, 247, 684
Macri, L. M., Stanek, K. Z., Bersier, D., Greenhill, L. J., & Reid, M. J. 2006, ApJ, 652, 1133
Madore, B. F. 1982, ApJ, 253, 575
Madore, B. F., & Freedman, W. L. 1991, PASP, 103, 933
Madore, B. F., & Freedman, W. L. 2009, ApJ, 696, 1498
Mager, V. A., Madore, B. F., & Freedman, W. L. 2013, ApJ, 777, 79
Marconi, M., et al. 2003, ApJ, 596, 299
Marconi, M., Fiorentino, G., & Caputo, F. 2004, A&A, 417, 1101
Marconi, M., & Clementini, G. 2005, AJ, 129, 2257
Marconi, M., Musella, I., Fiorentino, G., 2005, ApJ, 632, 590
Marconi, M., Bono, G., Caputo, F., et al. 2006, MmSAI, 77, 67
Marconi, M., & Degl'Innocenti, S. 2007, A&A, 474, 557
Marconi, M., & Di Criscienzo, M. 2007, A&A, 467, 223
Marconi, M. 2009, MmSAI, 80, 141

Marconi, M., Musella, I., Fiorentino, G., et al. 2010, ApJ, 713, 615
Marconi, M., Bono, G., Caputo, F., et al. 2011, ApJ, 738, 111
Marconi, M. 2012, Memorie della Societa Astronomica Italiana Supplementi, 19, 138
Marconi, M., Molinaro, R., Bono, G., et al. 2013, ApJ, 768, L6
Marconi, M., Musella, I., Di Criscienzo, M., et al. 2014, MNRAS, 444, 3809
Marconi, M. 2015, MmSAI, 86, 190
Marconi, M., Coppola, G., Bono, G., et al. 2015, ApJ, 808, 50
Marengo, M., Evans, N. R., Barmby, P., et al. 2010, ApJ, 709, 120
McNamara, D. H., Clementini, G., & Marconi, M. 2007, AJ, 133, 2752
Moretti, M. I., Dall'Ora, M., Ripepi, V., et al. 2009, ApJ, 699, L125
Muraveva, T., Palmer, M., Clementini, G., et al. 2015, ApJ, 807, 127
Musella, I., Ripepi, V., Clementini, G., et al. 2009, ApJ, 695, L83
Musella, I., Ripepi, V., Marconi, M., et al. 2012, ApJ, 756, 121
Natale, G., Marconi, M., & Bono, G. 2008, ApJ, 674, L93
Newman, J. A., Ferrarese, L., Stetson, P. B., et al. 2001, ApJ, 553, 562
Ngeow, C.-C., Kanbur, S. M., Nikolaev, S., et al. 2005, MNRAS, 363, 831
Ngeow, C., & Kanbur, S. M. 2008, ApJ, 679, 76
Ngeow, C.-C., et al. 2009, ApJ, 693, 691
Ngeow, C.-C., & Kanbur, S. M. 2010, ApJ, 720, 626
Ngeow, C.-C., et al. 2012, ApJ, 745, 104
Oey, M. S., & Kennicutt, R. C., Jr. 1993, ApJ, 411, 137
Olech, A., Dziembowski, W. A., Pamyatnykh, A. A., et al. 2005, MNRAS, 363, 40
Oluseyi, H. M., Becker, A. C., Culliton, C., et al. 2012, AJ, 144, 9
Phillips, M. M. 1993, ApJ, 413, L105
Pietrzyński, G., Gieren, W., Soszyński, I., et al. 2006, ApJ, 642, 216
Pietrzyński, G., Gieren, W., Soszyński, I., et al. 2006, AJ, 132, 2556
Pietrzyński, G., Thompson, I. B., Gieren, W., et al. 2010, Nature, 468, 542
Pojmanski, G. 2002, Acta Astronomica, 52, 397
Poleski, R., Soszyński, I., Udalski, A., et al. 2010, AcA, 60, 179
Rey, S.-C., Lee, Y.-W., Joo, J.-M., Walker, A., & Baird, S. 2000, AJ, 119, 1824
Richardson, J. C., Irwin, M. J., McConnachie, A. W., et al. 2011, ApJ, 732, 76
Riess, A. G., Macri, L., Li, W., et al. 2009, ApJS, 183, 109
Riess, A. G., Macri, L., Casertano, S., et al. 2009, ApJ, 699, 539
Riess, A. G., Macri, L., Casertano, S., et al. 2011, ApJ, 730, 119
Ripepi, V., Moretti, M. I., Marconi, M., et al. 2012, MNRAS, 424, 1807
Ripepi, V., Moretti, M. I., Marconi, M., et al. 2015, MNRAS, 446, 3034
Rizzi, L., Tully, R. B., Makarov, D., et al. 2007, ApJ, 661, 815
Romaniello, M., Primas, F., Mottini, M., et al. 2005, A&A, 429, L37
Romaniello, M., Primas, F., Mottini, M., et al. 2008, A&A, 488, 731
Saha, A., Sandage, A., Tammann, G. A., et al. 2001, ApJ, 562, 314
Sakai, S., et al. 2004, ApJ, 608, 42
Sandage, A., Tammann, G. A., & Reindl, B. 2004, A&A, 424, 43
Santolamazza, P., Marconi, M., Bono, G., et al. 2001, ApJ, 554, 1124
Sasselov, D. D., Beaulieu, J. P., Renault, C., et al. 1997, A&A, 324, 471
Searle, L., & Zinn, R. 1978, ApJ, 225, 357
Sollima, A., Cacciari, C., Arkharov, A. A. H., et al. 2008, MNRAS, 384, 1583
Soszynski, I., Poleski, R., Udalski, A., et al. 2008, AcA, 58, 163
Soszyński, I., Udalski, A., Szymański, M. K., et al. 2008, AcA, 58, 293
Soszyński, I., Udalski, A., Szymański, M. K., et al. 2009, AcA, 59, 1
Soszyński, I., Udalski, A., Szymański, M. K., et al. 2009, AcA, 59, 239
Soszyński, I., Udalski, A., Szymański, M. K., et al. 2010, AcA, 60, 165
Soszyński, I., Dziembowski, W. A., Udalski, A., et al. 2011, AcA, 61, 1
Soszyński, I., Udalski, A., Szymański, M. K., et al. 2014, AcA, 64, 177

Storm, J., Carney, B. W., Gieren, W. P., et al. 2004, A&A, 415, 521
Subramaniam, A., & Subramanian, S. 2009, A&A, 503, L9
Szewczyk, O., Pietrzyński, G., Gieren, W., et al. 2008, AJ, 136, 272
Storm, J., Gieren, W., Fouqué, P., et al. 2011, A&A, 534, A95
Tammann, G. A., & Reindl, B. 2002, Ap&SS, 280, 165
Tisserand, P., Le Guillou, L., Afonso, C., et al. 2007, A&A, 469, 387
Udalski, A., et al. 2008, AcA, 58, 69
Udalski, A., Szymański, M. K., & Szymański, G. 2015, AcA, 65, 1
van Albada, T. S., & Baker, N. 1971, ApJ, 169, 311
VandenBerg, D. A., et al. 2013, ApJ, 775, 134
Vivas, A. K., & Zinn, R. 2006, AJ, 132, 714
Wood, P. R., S. Arnold, A., & Sebo, K. M. 1997, ApJ, 485, L25
Zaritsky, D., Kennicutt, R. C., Jr., & Huchra, J. P. 1994, ApJ, 420, 87
Zinn, R., Horowitz, B., Vivas, A. K., et al. 2014, ApJ, 781, 22